

High-frame-rate observation of single femtosecond laser pulse propagation in fused silica using an echelon and optical polarigraphy technique

Xiaofang Wang,^{1,2} Lihe Yan,^{1,*} Jinhai Si,¹ Shigeki Matsuo,² Huailiang Xu,³ and Xun Hou¹

¹Key Laboratory for Physical Electronics and Devices of the Ministry of Education & Shaanxi Key Lab of Information Photonic Technique, Collaborative Innovation Center of Suzhou Nano Science and Technology, School of Electronics & Information Engineering, Xi'an Jiaotong University, Xianing-xilu 28, Xi'an 710049, China

²Department of Optical Science and Technology, The University of Tokushima, 2-1 Minamijosanjimacho, Tokushima 770-8506, Japan

³State Key Laboratory on Integrated Optoelectronics, College of Electronic Science and Engineering, Jilin University, 2699 Qianjin Street, Changchun 130012, China

*Corresponding author: liheyang@mail.xjtu.edu.cn

Received 25 August 2014; revised 4 November 2014; accepted 17 November 2014; posted 18 November 2014 (Doc. ID 221554); published 15 December 2014

We have demonstrated high-frame-rate observations of a single femtosecond laser pulse propagating in transparent medium using the optical polarigraphy technique and an echelon. The echelon produced a spatially encoded time delay for the probe pulse to capture directly four successive images of an intense propagating pulse with picosecond time interval and femtosecond time resolution. Using this method, we observed the propagation process of a single femtosecond laser pulse in fused silica. The influence of pulse-energy fluctuation on the spatial and temporal distribution of the single laser pulse was visualized using the single-shot measurements. © 2014 Optical Society of America

OCIS codes: (320.2250) Femtosecond phenomena; (190.3270) Kerr effect; (190.5530) Pulse propagation and temporal solitons; (320.7100) Ultrafast measurements.

<http://dx.doi.org/10.1364/AO.53.008395>

1. Introduction

Since the advent of the femtosecond laser, various methods have been developed to research the propagation behaviors of intense laser pulses in transparent media [1–7]. The femtosecond time-resolved optical polarigraphy (FTOP) technique, based on the optical Kerr effect, can be used to directly observe the instantaneous intensity distributions of optical pulses propagating with two-dimensional spatial distribution [8–10]. Since the intense laser pulses develop complex structures during their propagation

arising from self-modulation due to nonlinear effects [11], the propagation profile is quite different from shot to shot, even if the laser light source fluctuates slightly. As the traditional FTOP method is conventionally conducted with a pump pulse and a variably delayed probe pulse, with many repetitions of the pump–probe sequence, it is difficult to observe the instantaneous intensity distributions of a single laser pulse at several successive temporal points.

To fulfill the single-shot detection of the intense laser pulse propagation, Fujimoto *et al.* installed a quadruple-pulse generator in the optical path and realized a successive four-frame instantaneous observation of an intense pulse propagating in air [10]. However, the quadruple-pulse generator, which

combines four different probe beams with different optical paths, will largely increase the complexity of the experiments. Some other single-shot imaging techniques, such as tomography [12,13] and x-ray diffraction [14,15] methods, have been proposed to visualize ultrafast phenomena. For example, Matlis *et al.* observed the structure and position information for laser-induced plasma filaments using a single-shot ultrafast tomographic imaging by spectral multiplexing [12]. In our previous work, we demonstrated a simple multiframe observation method of a femtosecond laser pulse propagating in transparent medium based on an echelon and the FTOP technique [16]. A stair-step echelon [17–19] was introduced into the probe light and divided it into multipulse both in time and space, allowing a multiframe detection of the intense laser pulse propagating in materials. Using this method, we realized a four-frame observation of a single femtosecond laser pulse propagating in CS₂ easily. However, because of the slow time response of the Kerr medium CS₂, the probe light in the femtosecond regime would sense the residual birefringence of the pump light, thereby reducing the temporal resolution as well as the frame rate of the imaging.

In this paper, we observed the propagation dynamics of femtosecond laser pulses in fused silica using the single-shot measurements based on FTOP and an echelon. As the material had an ultrafast nonlinear response, the temporal resolution of the imaging in fused silica was mainly limited by the pulse duration, and the frame rate of the imaging could be higher than 1 THz. Using this method, we observed the propagation process of a single femtosecond laser pulse in fused silica. The influence of pulse-energy fluctuation on the spatial and temporal distribution of the single laser pulse was visualized using the single-shot measurements.

2. Experiments

Figure 1 illustrates the experimental setup. The experiments were performed using 65 fs, 800 nm pulses from a regeneratively amplified Ti:sapphire laser system (Libra-USP-HE, Coherent Inc.) operating at 1 kHz repetition rate. The laser beam was split into a pump and a probe beam by a beam splitter. After passing through a delay line, the polarization of the pump beam was changed to vertical using a half-wave plate. The pump beam was focused into a 10-mm long Kerr medium of fused silica glass by a lens of 100-mm focal length. The nonlinear focus of the pump beam was located at about 1 mm inside the input surface of the samples. To avoid the background scattering of the pump light, the probe beam was frequency doubled to 400 nm by a 1-mm thick β -barium borate crystal. Then it was calibrated by a confocal lens and passed through a stair-step echelon, which separated the probe light in space and time. The modulated probe beam was then introduced into the Kerr medium perpendicularly to the direction of the pump path, with the light spot covering

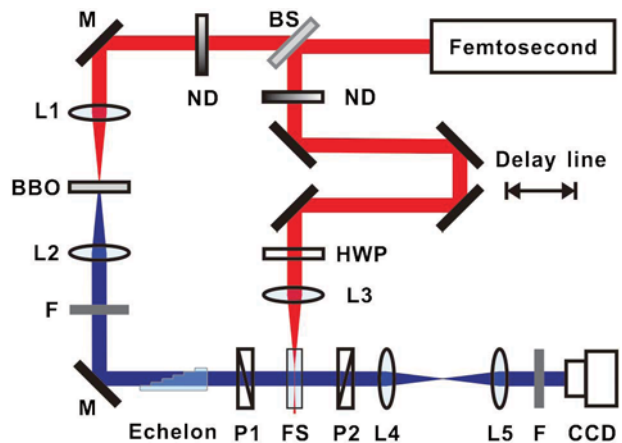


Fig. 1. Experimental setup of multiframe FTOP imaging technique using an echelon. BS, beam splitter; ND, neutral density filter; M, mirror; L, lens; FS, fused silica; P, polarizer; HWP, half-wave plate.

the area of the focal point of the pump beam. In front of fused silica, a polarizer (P1) was set to 45 deg with respect to the horizontal plane of the optical stage and allowed parts of the probe light to pass. When the pulse passed through the interaction region, only the components perpendicular to the polarizer could be extracted by the analyzer (P2) placed behind the sample. To record the polarigraphy image, a high-spatial-resolution charge coupled device (CCD) camera was located on the imaging plane of the pump light path.

The echelon with four steps is mechanically fabricated on a microscope cover glass. The step width is about 0.54 mm, producing a time delay of about 0.96 ps for 400 nm probe pulse ($n = 1.53$). As each step produces one frame of the FTOP image, the introduced delay time by each step must agree with the propagation time of the 800 nm pump pulse in fused silica ($n = 1.45$). Hence, the height of the step is designed to be about 0.2 mm [$\approx 0.96 \text{ ps} \times (c/1.45)$, $c = 3.0 \times 10^8 \text{ m/s}$].

3. Results and Discussion

Figure 2 shows the recorded four-frame instantaneous FTOP image of 15 μJ pump pulse propagating in fused silica. The pulse propagated from the left to right. The exposure time of the CCD camera was

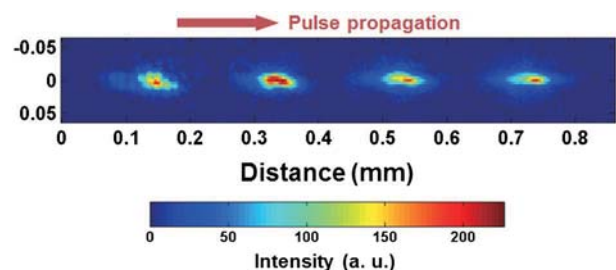


Fig. 2. Four-frame observation of pulse propagation in fused silica using 100 pulses of 15 μJ . The pulse propagated from left to right.

set at 100 ms and 100 pulses were used to produce the image. The spatial resolution of the image is estimated to be $4.3\ \mu\text{m}$. The image has four profiles, each corresponding to one frame of the temporal intensity distributions of the laser pulse propagating in fused silica at different times. The interval between the peaks of adjacent profiles was $0.96\ \text{ps}$ in time, correspondingly $0.2\ \text{mm}$ in space, which was decided by the step width of the echelon. As each stair of the echelon had different thickness and transmittance, and the probe pulse intensity distribution was not strictly uniform, each frame of the FTOP image was normalized by comparing with the intensity distribution of the incident probe pulse after passing through the echelon. From the figure we can see that the lateral size of the pump light spot changed slightly inside the sample even after the lens focus locating at $1\ \text{mm}$ inside the sample. Because of the balance between the Kerr self-focusing and plasma defocusing effect induced by the nonlinear ionization, a filament was produced inside fused silica [20].

In the FTOP measurements, the probe pulse collides with the pump pulse while running through each other in the medium. If the radius of the pump beam and the nonlinear response of the material are finite, the temporal resolution of the imaging is determined only by the convolution of the probe pulse and the square of the integral of the intensity of the pump pulse [21]. For further analysis, we acquired the exposure intensity distribution along the propagating axis of the FTOP profiles given in Fig. 2. The squares in Fig. 3 show the acquired intensity distributions as a function of the propagating time of the pump pulse. The red solid curves indicate Gaussian fits of the image intensity for each frame with the full-width at half-maximum (FWHM) of $276\ \text{fs}$. This value is absolutely larger than the FWHM of the convolution of the probe pulse and the square of the pump light intensity. In our experiments, the origin of the nonlinear response of the material is mainly attributed to electronic process, the characteristic

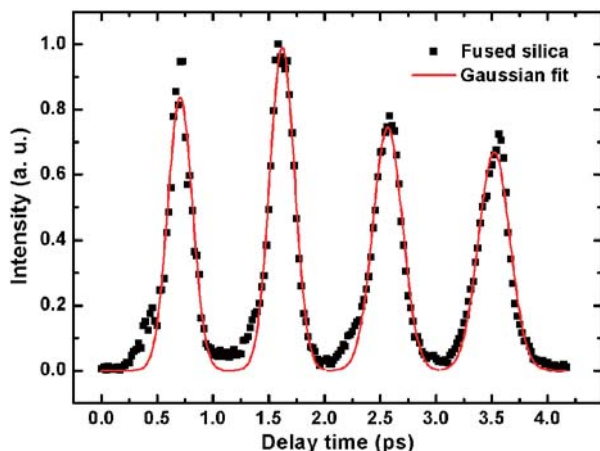


Fig. 3. Exposure intensity distribution of the four-frame FTOP image as a function of the propagation time of the pump pulse. The solid lines show the Gaussian fit curves.

time of which is much faster than the pulse duration. Hence, the influence of the nonlinear response of the material on the temporal resolution of the imaging could be neglected. The measured pump beam diameter is estimated to be about $40\ \mu\text{m}$. By considering the linear refractive index of the material, the interacting time of the pump and probe pulses is elongated by about $190\ \text{fs}$. Hence, the temporal resolution of the imaging is limited by the pulse duration and the lateral size of the pump beam in the sample.

The frame interval was estimated to be about $0.96\ \text{ps}$, corresponding to a frame rate of about $1.05\ \text{THz}$. It is much higher than $0.25\ \text{THz}$ frame rate in CS_2 which we have obtained in previous work [16]. It should be noted that the intensity of the image after the second frame became lower, as shown by Figs. 2 and 3. This was caused by the pump pulse energy reduction. The pump pulse energy might be absorbed by multiphoton absorption, or be refracted by ionization-induced refraction during the filamentation process in fused silica [11].

Then, we observed the propagation dynamics of a single laser pulse in fused silica in Fig. 4(a). The CCD exposure time was set to $1\ \text{ms}$ enabling single-shot recording. The pump pulse energy was increased to $45\ \mu\text{J}$ to enhance the signal-to-noise ratio of the imaging. Similarly to Fig. 3, the interval between the two adjacent profiles of the image was fixed at $0.2\ \text{mm}$. Propagation profiles under the same experimental conditions but for different laser shots are shown in Figs. 4(b)–4(d). These profiles are different from each other, which might be resulted from the pulse energy fluctuation. For example, the intensity of Fig. 4(a) is much higher than the other three. Meanwhile, the spatial and temporal positions of the most intense part of each pulse propagating in the fused silica are also different from shot to shot

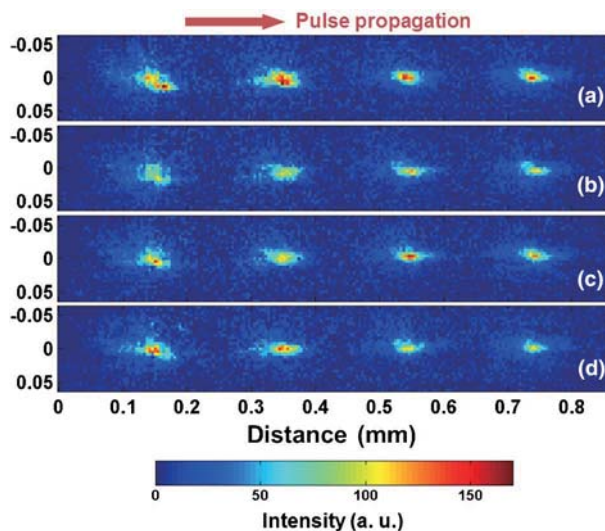


Fig. 4. Single-shot four-frame observation of single $45\ \mu\text{J}$ pulse propagation in fused silica. The pulse propagated from left to right. (a)–(d) correspond to different laser shots under the same conditions.

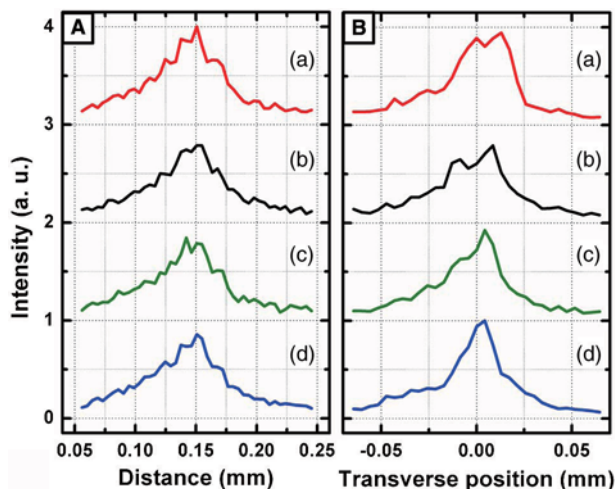


Fig. 5. Intensity distributions of the first frames of the single-shot images shown in Figs. 4(a)–4(d). (A) Along the pulse propagation direction and (B) along the transverse direction.

due to the pulse energy distribution fluctuation at incidence.

Furthermore, we analyzed the intensity distributions of the single-shot images of the first frames shown in Figs. 4(a)–4(d). Figure 5(A) shows the intensity distributions of the images along the pulse propagation direction. From the figure we can see that the peak intensity of the pulse fluctuates from shot to shot. Compared with the maximum peak in (a), the peak intensity of (b) is about 21% lower. The influence of the instability of the CCD exposure intensity could be ruled out, as the pulse-to-pulse energy stability of the pump pulse energy was measured to be 0.45% rms. Since the intense pump pulse might develop complex structures during their propagation arising from self-modulation due to nonlinear effects [11], the propagation profile is quite different from shot to shot, even if the laser light source fluctuates slightly. Figure 5(B) shows transverse intensity distributions of the corresponding single pulse. It can be clearly seen that transverse modes of the four pulses differ a lot from each other. Two peaks are observed in pulses (a) and (b), indicating that two filaments were formed when the pulse propagated in fused silica.

4. Conclusion

In conclusion, we have performed a successive four-frame instantaneous observation of single femtosecond laser pulse propagation in fused silica using an echelon combined with FTOP. Because of the ultrafast response of fused silica, the temporal resolution of the imaging is limited mainly by the probe pulse duration. The interval between adjacent frames is about 0.96 ps, corresponding to a frame rate of about 1.05 THz, which is much higher than 0.25 THz obtained in our previous works in CS₂. From the single-shot images, we can directly observe the shot-to-shot variations of the pump pulse propagation profiles caused by the pulse energy fluctuation.

This work was partially supported by the National Basic Research Program of China (973 Program) under grant 2012CB921804, the National Natural Science Foundation of China (NSFC) under the grants 61235003, No. 11304242, and Opened Fund of the State Key Laboratory on Integrated Optoelectronics No. IOSKL2012KF.

References

1. C. E. Clayton, K.-C. Tzeng, D. Gordon, P. Muggli, W. B. Mori, C. Joshi, V. Malka, Z. Najmudin, A. Modena, D. Neely, and A. E. Dangor, "Plasma wave generation in a self-focused channel of a relativistically intense laser pulse," *Phys. Rev. Lett.* **81**, 100–103 (1998).
2. S. Minardi, A. Gopal, M. Tatarakis, A. Couairon, G. Tamošauskas, R. Piskarskas, A. Dubietis, and P. D. Trapani, "Time-resolved refractive index and absorption mapping of light-plasma filaments in water," *Opt. Lett.* **33**, 86–88 (2008).
3. T. Balciunas, A. Melninkaitis, G. Tamosauskas, and V. Sirutkaitis, "Time-resolved off-axis digital holography for characterization of ultrafast phenomena in water," *Opt. Lett.* **33**, 58–60 (2008).
4. M. Centurion, Y. Pu, and D. Psaltis, "Holographic capture of femtosecond pulse propagation," *J. Appl. Phys.* **100**, 063104 (2006).
5. T. Kubota, K. Komai, M. Yamagiwa, and Y. Awatsuji, "Moving picture recording and observation of three-dimensional image of femtosecond light pulse propagation," *Opt. Express* **15**, 14348–14354 (2007).
6. A. Mermillod-Blondin, C. Mauchair, J. Bonse, R. Stoian, E. Audouard, A. Rosenfeld, and I. V. Hertel, "Time-resolved imaging of laser-induced refractive index changes in transparent media," *Rev. Sci. Instrum.* **82**, 033703 (2011).
7. S. L. Chin, S. A. Hosseini, W. Liu, Q. Luo, F. Théberge, N. Aközbek, A. Becker, V. P. Kandidov, O. G. Kosareva, and H. Schroeder, "The propagation of powerful femtosecond laser pulses in optical media: physics, applications, and new challenges," *Can. J. Phys.* **83**, 863–905 (2005).
8. M. Fujimoto, S. Aoshima, M. Hosoda, and Y. Tsuchiya, "Femtosecond time-resolved optical polarigraphy: imaging of the propagation dynamics of intense light in a medium," *Opt. Lett.* **24**, 850–852 (1999).
9. M. Fujimoto, S. Aoshima, and Y. Tsuchiya, "Ultrafast imaging to measure instantaneous intensity distributions of femtosecond optical pulses propagating in a medium," *Meas. Sci. Technol.* **13**, 1698–1709 (2002).
10. M. Fujimoto, S. Aoshima, and Y. Tsuchiya, "Multiframe observation of an intense femtosecond optical pulse propagating in air," *Opt. Lett.* **27**, 309–311 (2002).
11. A. Couairon and A. Mysyrowicz, "Femtosecond filamentation in transparent media," *Phys. Rep.* **441**, 47–189 (2007).
12. N. H. Matlis, A. Axley, and W. P. Leemans, "Single-shot ultrafast tomographic imaging by spectral multiplexing," *Nat. Commun.* **3**, 1111 (2012).
13. Z. Li, R. Zgadzaj, X. Wang, Y. Chang, and M. C. Downer, "Single-shot tomographic movies of evolving light-velocity objects," *Nat. Commun.* **5**, 3085 (2014).
14. A. Barty, S. Boutet, M. J. Bogan, S. Hau-Riege, S. Marchesini, K. Sokolowski-Tinten, N. Stojanovic, R. Tobey, H. Ehrke, A. Cavalleri, S. Düsterer, M. Frank, S. Bajt, B. W. Woods, M. M. Seibert, J. Hajdu, R. Treusch, and H. N. Chapman, "Ultrafast single-shot diffraction imaging of nanoscale dynamics," *Nat. Photonics* **2**, 415–419 (2008).
15. T. Wang, D. Zhu, B. Wu, C. Graves, S. Schaffert, T. Rander, L. Müller, B. Vodungbo, C. Baumier, D. P. Bernstein, B. Bräuer, V. Cros, S. Jong, R. Delaunay, A. Fognini, R. Kukreja, S. Lee, V. López-Flores, J. Mohanty, B. Pfau, H. Popescu, M. Sacchi, A. B. Sardinha, F. Sirotti, P. Zeitoun, M. Messerschmidt, J. J. Turner, W. F. Schlotter, O. Hellwig, R. Mattana, N. Jaouen, F. Fortuna, Y. Acremann, C. Gutt, H. A. Dürr, E. Beaurepaire, C. Boeglin, S. Eisebitt, G. Grübel, J. Lüning, J. Stöhr, and A. O. Scherz, "Femtosecond single-shot imaging of nanoscale

- ferromagnetic order in Co/Pd multilayers using resonant x-ray holography," *Phys. Rev. Lett.* **108**, 267403 (2012).
16. L. Yan, X. Wang, J. Si, P. He, F. Chen, J. Zou, and X. Hou, "Multi-frame observation of a single femtosecond laser pulse propagation using an echelon and optical polarigraphy technique," *IEEE Photon. Technol. Lett.* **25**, 1879–1881 (2013).
 17. P. R. Poulin and K. A. Nelson, "Irreversible organic crystalline chemistry monitored in real time," *Science* **313**, 1756–1760 (2006).
 18. H. Sakaibara, Y. Ikegaya, I. Katayama, and J. Takeda, "Single-shot time-frequency imaging spectroscopy using an echelon mirror," *Opt. Lett.* **37**, 1118–1120 (2012).
 19. Y. Minami, Y. Hayashi, J. Takeda, and I. Katayama, "Single-shot measurement of a terahertz electric-field waveform using a reflective echelon mirror," *Appl. Phys. Lett.* **103**, 051103 (2013).
 20. A. Couairon, L. Sudrie, M. Franco, B. Prade, and A. Mysyrowicz, "Filamentation and damage in fused silica induced by tightly focused femtosecond laser pulses," *Phys. Rev. B* **71**, 125435 (2005).
 21. M. Fujimoto, S. I. Aoshima, M. Hosoda, and Y. Tsuchiya, "Analysis of instantaneous profiles of intense femtosecond optical pulses propagating in helium gas measured by using femtosecond time-resolved optical polarigraphy," *Phys. Rev. A* **64**, 033813 (2001).